FATIGUE OF GROUTED JOINT CONNECTIONS

Prof. Peter Schaumann, Dipl.-Ing. Fabian Wilke
ForWind – Center for Wind Energy Research
Institute for Steel Construction, Leibniz University of Hannover,
Appelstr. 9A, 30167 Hannover, Germany
+49-511-762-3367; wilke@stahl.uni-hannover.de

1 Introduction

"Grouted Joint" connections - well known in oil and petroleum industry - also have been used in Monopile-foundations for offshore wind energy converters (OWECS) in the last decade. It is common practice in offshore wind energy industry to use high performance concrete (HPC) for the grouted connections. So far little knowledge exists regarding the fatigue characteristics of the brittle grout material itself and of the whole connection under predominating bending. Furthermore the geometrical parameters of current support structures lie outside the range of the tests performed in the past. In design practice this lack of knowledge leads often to a very conservative dimensioning and design.
For that reason a research project has been initiated which includes scale tests of grouted joints to study their load bearing and fatigue behaviour. Furthermore the results allow an adjustment and validation of applied material models.

2 Test results

The tests – performed on the specimens with the dimensions given in Table 1 – have been carried out with and without shear keys. For the grout a HPC with a compressive strength of about 130 N/mm² (see Table 2) has been used.

Small Scale tests		Large Scale Tests	
D_p [mm]	60.3	D_p [mm]	800
D_p/t_p [-]	5.5	D_p/t_p [-]	100
t_g [mm]	19	t_g [mm]	20
D_s/t_s [-]	14.3	D_s/t_s [-]	107
L_g	1.5 x D_p	L_g	1.3 x D_p

Table 1: Geometric parameters of the test specimen

As stated in the standards [1],[2] the ultimate load of the connection strongly increases with application of shear keys. Due to the additional mechanical interlock the load carrying behaviour changes from a frictional type to a strut and tie model. Two typical load-displacement curves are displayed in Figure 1. The kink in the curve of the specimen with shear keys at about 50% of the ultimate load is caused by transverse cracking of the bottom compression strut. In terms of the large displacements at fracture, which are in the size of 1.5% of the length of the grout, it seems reasonable to define the maximum load conservatively at a level near the first crack. This is particularly valid for structures with alternating axial forces (Tripods, Jackets).

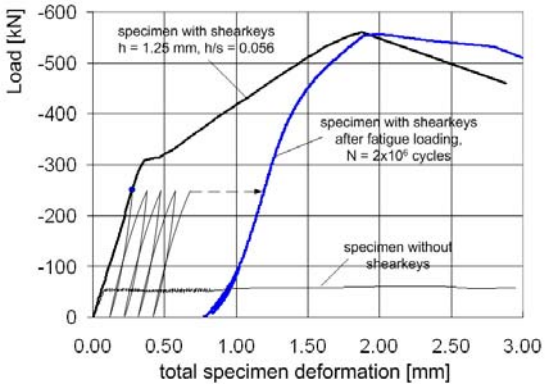

Figure 1: Load-displacement curves for the different small scale specimen

Comparison with the regulations of Det Norske Veritas shows that the characteristic values of the test for the specimen with shear keys are slightly lower (-9%). Due to the big scatter in results for the specimen without shear keys, which is typical for imperfection driven load-carrying mechanisms, the characteristic capacities lie far below the recommendations of [1],[2]. The tested capacities are even reduced if the bending moments due to imperfections of the loading platens are excluded by numerical analysis. Thus, from the knowledge gained so far, the authors recommend to apply additional mechanical interlock (e.g. shear keys) also for monopile structures with relatively low axial forces.
In addition to the static tests the specimens have been loaded dynamically with an upper load level of 256 kN (for the connection with shear keys) which equals a stress range of over 140 N/mm² in the pile section. Even after 2 Million cycles the specimens nearly reach the load of the static test (Figure 1). This behaviour is in compliance with the energy based model in [3], as the dissipated energy during fatigue loading is less than the energy contained in the static envelope. The local deterioration around the shear keys with simulated damage values D>1 does not reduce the 'global' capacity.
With regard to a FE-based design procedure this means that the localized damage around the shear keys need not to be considered in the global analysis without loosing to much accuracy.

f_{cm}	f_{ck}	f_t	E	υ
[N/mm²]	[N/mm²]	[N/mm²]	[N/mm²]	[-]
133	123	7	50000	0.19

Table 2: Material properties of the DENSIT S5 material used for the tests

3 Numerical Investigations

3.1 Material model and damage

For the choice of the adequate material model for the HPC it has to be distinguished between

- local models, which are used to analyse the material behaviour around the shear keys
- global models like the large scale grouted joint.

Due to the confinement together high stress concentrations large hydrostatic pressures occur at the shear keys. Furthermore, most of the stress states of the nodes in the process zone lie close to the tensile meridian of the HAIGH-WESTERGAARD space. Figure 2 shows the angle of similarity θ in the octahedral plane for the elements close to the shear keys. A concentration of the frequency in the region between 0° - 30° can be recognised.

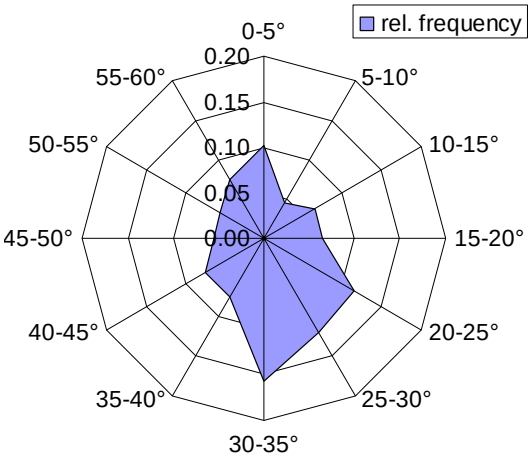

Figure 2: Frequency of different angles of similarity θ of the HAIGH-WESTERGAARD space for the elements in the process zone around the small scale shear keys

Therefore multi-parameter fracture surfaces, e.g. the OTTOSEN model, recommended by CEB-FIP [4], have to be used, as simple models like the DRUCKER-PRAGER underestimate the strains under these conditions.

To reduce calculation time for time domain analysis, the following approach is chosen:

- The transfer function including geometric and material nonlinearities is determined be FE-calculation.
- For a given time series the damage and the stiffness degradation at each node is calculated using a degradation formula either based on the work in [3] or [5]. The damaged stiffness matrix is updated using the scalar damage approach:

$$E_i = (1 - D) \cdot E_0 \qquad (1)$$

This procedure brings along the assumption that the stiffness of the structure stays constant over a certain range of cycles, thus reducing the calculation time.

The results of the numerical fatigue simulation for the small scale specimen has been compared to a simple linear damage approach without stiffness degradation in Figure 3.

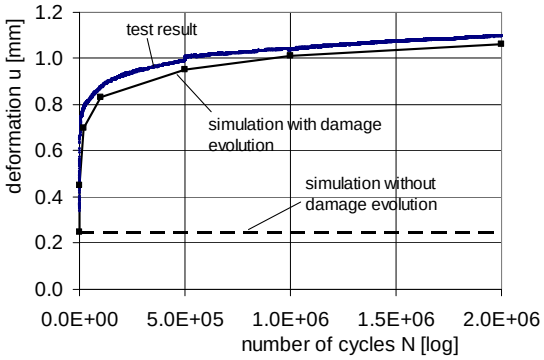

Figure 3: Development of total deformation during the fatigue test of the small scale specimen

The stress state in the 'global' structure is less sensitive to the material model as the stresses are low at fatigue level. For the calculations of the large scale structures of the following chapters a DRUCKER-PRAGER failure surface has been used in conjunction with a stiffness degradation function defined in [5]. The damage evolution is assumed to be linear. It has to be noted that the application of the Miner rule is accepted for random loading with spectra shown in Figure 9. For block loading, other approaches, e.g. energy based ones [3], have to be used (see e.g. [6]).

3.2 Example structure

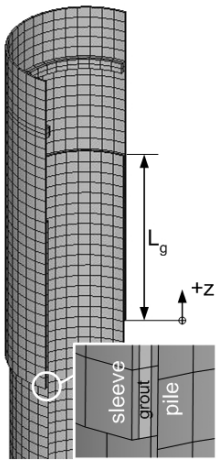

Grouted Joint

D_p =	5000 mm
D_p/t_p =	100
D_s/t_s =	105
t_{grout} =	90 mm
L_g = 1.5/1.25/1.0 * D_p	

Turbine

Output:	4 MW
Mass:	280 t
Hub height:	69 m (LAT)

Tower

1st EF:	0.29 Hz

Figure 4: Reference structure at a Baltic Sea location

The developed models are applied to a reference structure with the FE-System and the main parameters shown in Figure 4. As it is an Baltic Sea location (water depth 18 m) with moderate extreme wave heights, the platform level and the ringflange are close to the grouted joint connection and have to be considered in the model. The slenderness ratios of the pile are equal to those of the large scale tests (Table 1). The stress-strain relation of steel is implemented with a standard bilinear curve.

To account for thickness effects the compression strength f_{ck} of Table 2 has been multiplied with a factor 0.91 derived from the Multifractal Scaling Law (MFSL), see [7]. As the calculated damage in the concrete is low, the further examination will focus on the damage of the pile section at the transition piece.
The calculated damage for the steel structure is evaluated at each node based on the stress history of the normal stress components of rotating planes. The stress transformation for each plane is done by multiplying the stress tensor with the Euler-angle transformation matrices.
The fatigue classes for the design have been assumed as defined in Table 3. The reduced FAT-class for the inside covers any welded attachments.

	inside	outside
FAT	71	112
inspection possible?	yes	no
corrosive environment	no	yes

Table 3: Definition of detail classes and environmental conditions for the pile section

Figures 5 and 6 contain a developed view of the damages around the circumference. It should be noted that the FE-coordinate system has been rotated with 90° compared to the standard wind energy coordinate system (see Figure 9). Therefore the maximum damages occur at the opposite meridians at 90°/270°, as the bending moment is broken up into a couple of forces. The maximum damage on the critical planes orthogonal to the z-direction occurs at the transition grout to pile. It is caused by the forming buckle which also governs the ultimate limit state design (Figure 5)
Comparison with the damage due to circumferential stresses caused by ovalisation at the other end of the connection illustrates that the latter govern the design (Figure 6). It is important especially for the conceptual design phase that the increase in damage is dramatic (Figure 7). Compared to the effects of the shorter overlap length on the longitudinal stresses and the ultimate limit buckling state this is the actual design driver.

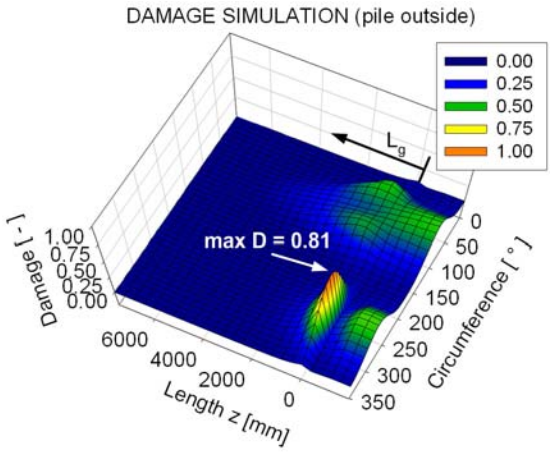

Figure 5: Developed view for the fatigue damage in the pile (L_g = 1.5 x D_p), stresses in longitudinal direction, outside of the pile

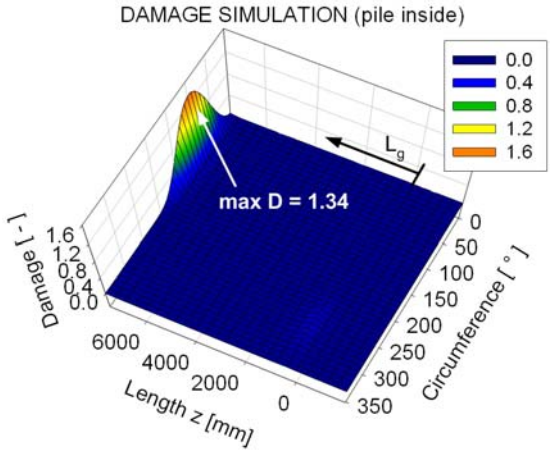

Figure 6: Developed view for the fatigue damage in the pile (L_g = 1.5 x D_p), stresses in circumferential direction, pile inside

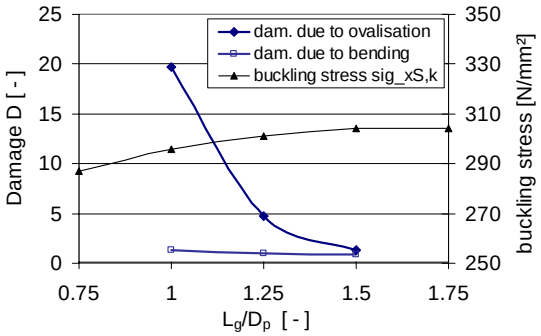

Figure 7: Influence of overlap length L_g/D_p on the fatigue damage and the buckling stresses

3.3 Effects of spatial loading

In contrast to the load transfer of the axially loaded connection the geometric nonlinearities due to contact mechanism in the grout-steel interface lead to a stress distribution that differs remarkably from a plain pile section (Figure 8). Against this background the spatial influences of the load time series, which are usually neglected due to the weak correlation of M_x and M_y, have to be analysed. In this three-dimensional case the transfer function for the stresses of each node is no more only dependent of the load but additionally of the angle of attack of the bending moment.

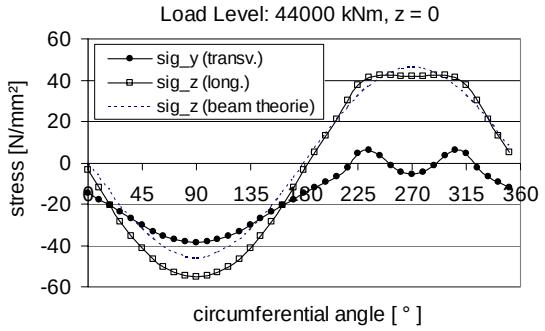

Figure 8: Transfer function for the stresses in longitudinal (σ_z) and circumferential direction (σ_y) compared to the one of a plain pile, location z = 0

The time series used for the simulation contain bending moments M_x and M_y. The waves have been simulated unidirectional parallel to the thrust force F_x. Table 4 shows the maximum damage for a transition piece with overlap lengths of 1.0times and 1.5times the pile diameter.

		uni-directional	with spatial time histories
L_g/D_p = 1.5	Damage (long.)	0.88	0.87
	Damage (transv.)	1.35	1.34
L_g/D_p = 1.0	Damage (long.)	1.33	1.34
	Damage (transv.)	19.84	19.66

Table 4: Results of the simulation with and without spatial influences

The increase in damage and the spatial influences can be neglected. Nevertheless it must be stated that any reduction in damage, derived from wave spreading effects at pile sections, cannot be transferred to this connection. It is recommended not to take spreading effects into account for grouted joints without detailed simulation.

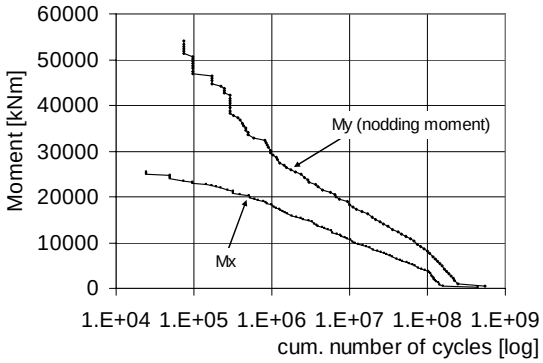

Figure 9: Load spectra for the given location

3.4 Nonlinearities and damage

For grouted joint connections with fatigue load spectra typical for wind energy converters the material laws for the global structural analysis of the steel structure can be linearised as already pointed out in section 3.2. Due to the low stresses in the grout material compared to its ultimate capacity nearly no nonlinear material behaviour occurs at the fatigue load level. A comparison of the fatigue damages for two systems is given in Table 5. System A contains only geometric nonlinearities (contact) whereas System B includes all the elements mentioned in section 3.1.

		Model A	Model B
L_g/D_p = 1.25	Damage (long.)	1.01	1.00
	Damage (transv.)	4.69	4.63

Table 5: Comparison of resulting maximum damage for the Model A without material nonlinearities and Model B with nonlinearities (concrete material and stiffness degradation)

3.5 Influence of shear keys

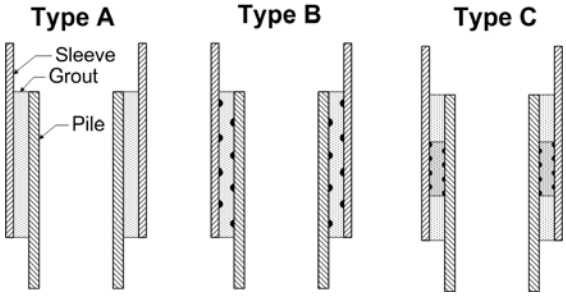

Figure 10: Monopile types in terms of axial load transfer mechanism (A: plain pipe; B: connection with shear keys; C: shear keys only in the center of the grout)

Besides the benefits of shear keys in resisting axial forces, their welding usually leads to sharp notches

together with distinct changes in local hardness and steels microstructure. Two possible configurations occur: shear keys as weld beads or fillet welded bars. The different types have been analysed with local concepts (see [8]) to derive a FAT-class for the shear keys. A comparison of the notch stress approach [9],[10] on the one hand and the notch strain approach plus fracture mechanics [11],[12] shows a good compliance. Table 6 summarises the derived FAT-classes.

weld bead	fillet welded bars	
-	root cracking	toe cracking
80 *(71)*	71	80

Table 6: FAT-classes for the structural detail 'shear key' (value in parethesis is for undercut > 0.5 mm)

If exemplarily the FAT-class 80 is applied to the fatigue design of the outside area of the pile it gets obvious that it is necessary to attach the shear keys only in the middle of the overlap length (~1/4th to 1/3rd of L_g, compare Type C in Figure 10). In doing so, a comparison of the fatigue envelope of the pile outside in Figure 11 with the original one in Figure 5 illustrates that any detrimental effect can be avoided. But for a lower FAT class the area of the shear keys would govern the design (D = 1.54 for FAT 71).

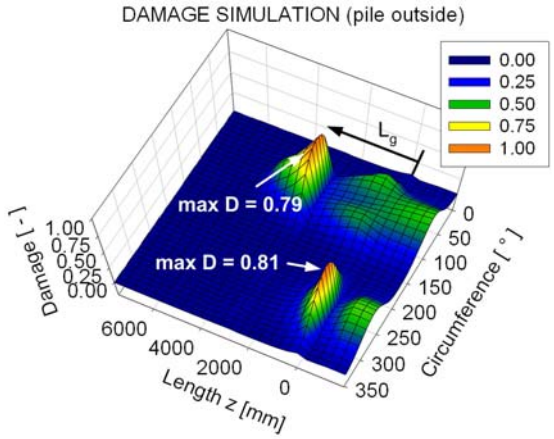

Figure 11: Developed view for the fatigue damage in the pile (L_g = 1.5 x D_p), stresses in longitudinal direction, pile outside

4 Summary

Based on their test experience the authors recommend the application of additional mechanical interlock even for structures with low axial forces. Fatigue tests on axially loaded specimen show that local deterioration of the HPC around the shear keys can be neglected for the global analysis.
For the numerical investigations the choice of the material models depends on the examined detail. For the design of the steel structure linearization of the concrete material is acceptable.
Fatigue design of a real structure demonstrates that pile ovalisation becomes design driver if a reduction of overlap length is intended.
A too penalizing effect of the application of shear keys can be avoided if they are placed in the center region of the grout.

5 Acknowledgement

The research programme ForWind (www.forwind.de) at the Universities of Hannover and Oldenburg is funded from 2003-2008 by the Federal Ministry for Science and Culture of Lower Saxony, Germany. The provision of material by DENSIT A/S, Vallourec & Mannesmann Tubes and SIAG Stahlbau AG is kindly acknowledged.

6 References

[1] Det Norske Veritas (ed) (2004): Design of Offshore Wind Turbine Structures, Offshore Standard DNV-OS-J101, Hovik, Norway
[2] N-004 (1998): Design of Steel Structures. NORSOK Standard
[3] Pfanner, D. (2003): Zur Degradation von Stahlbetonbauteilen unter Ermüdungs-beanspruchung. PhD-Thesis, Ruhr-Universität Bochum
[4] CEB-FIP (1993), Model Code 1990, Comité Euro-International du Béton, Thomas Telford Services Ltd, London
[5] Holmen, J. O. (1979): Fatigue of concrete by constant and variable amplitude loading, Bulletin No. 79-1, Division of Concrete Structures, NTH – Trondheim
[6] Grünberg J.; Göhlmann, J. (2006): Schädigungsberechnung an einem Spann-betonschaft für eine Windenergieanlage unter mehrstufiger Ermüdung. Beton- und Stahlbetonbau, Vol. 101, No. 8, pp. 557-570
[7] Carpinteri, A; Ferro, G. and Monetto, I. (1999): Scale effects in uniaxially compressed concrete specimens. Magazine of Concrete Research, Vol. 51, No. 3, pp. 217 - 225
[8] Radaj D.; Sonsino, C.M. (1998): Fatigue Assessment of Welded Joints by Local Approaches. Abbington Publishing, Cambridge
[9] Hobbacher, A. (1996): Fatigue design of welded joints and components. IIW Doc XIII-1539-96, Abbington Publishing, Cambridge
[10] Schaumann, P.; Wilke F. (2005): Current developments of support structures for wind turbines in offshore environment. In: Shen et. al (eds), Advances in Steel Structures, Elsevier Ltd., pp. 1107-1114
[11] Schaumann, P.; Wilke, F. (2006): Benefits of Fatigue Assessment with Local Concepts. In: Peinke et. al (eds), Wind Energy – Proceedings of the Euromech Colloquium, Springer, pp. 293-296
[12] Schaumann, P.; Wilke, F. (2006): Enhanced Structural Design for Offshore Wind Turbines. XICAT 2006, Xi'an International Conference of Architecture and Technology, Xi'an, China (to be published)